Accelerated dendritic-cell migration and T-cell priming in SPARC-deficient mice

Sabina Sangaletti[1], Lucia Gioiosa[1], Cristiana Guiducci[1], Gianluca Rotta[2], Maria Rescigno[2], Antonella Stoppacciaro[3], Claudia Chiodoni[1] and Mario P. Colombo[1],*

[1]Immunotherapy and Gene Therapy Unit, Department of Experimental Oncology, Istituto Nazionale per lo Studio e la Cura dei Tumori, 20133 Milano, Italy
[2]Department of Experimental Oncology, European Institute of Oncology, 20141 Milano, Italy
[3]Department of Experimental Medicine and Pathology, 2nd Faculty of Medicine, University of Rome "La Sapienza", Roma, Italy
*Author for correspondence (e-mail: mario.colombo@istitutotumori.mi.it)

Summary

On their path to draining lymph nodes, epidermal Langerhans cells traverse collagen-dense connective tissue before reaching lymphatic vessels. The matricellular protein SPARC (secreted protein, acidic and rich in cysteine), which is induced during inflammation and tissue repair, organizes collagen deposition in tissue stroma. We analyzed Langerhans cell and dendritic-cell migration and its impact on T-cell priming in SPARC-null (SPARC^{-/-}) and SPARC-sufficient (SPARC^{+/+}) mice. Although the same number of Langerhans cells populate the ear skin of SPARC^{-/-} and SPARC^{+/+} mice, more Langerhans cells were found in the lymph nodes draining antigen-sensitized ears of SPARC^{-/-} mice and significantly more Langerhans cells migrated from null-mice-derived ear skin explants. Such favored Langerhans cell migration is due to the host environment, as demonstrated by SPARC^{+/+}>SPARC^{-/-} and reciprocal chimeras, and have a profound influence on T-cell priming. Contact-, delayed type-hypersensitivity and naive T-cell receptor-transgenic T-cell priming, together indicate that the lack of SPARC in the environment accelerates the onset of T-cell priming by hastening Langerhans cell/dendritic-cell migration.

Supplementary material available online at
http://jcs.biologists.org/cgi/content/full/118/16/3685/DC1

Key words: DC migration, SPARC, T-cell priming

Introduction

Epidermal Langerhans cells (LCs) and dermal dendritic cells (DCs) are professional antigen-presenting cells (APCs) that reside in the skin. LCs capture and process epicutaneous antigen (Ag), and migrate to the regional lymph node (LN) through a well-described pathway (Austyn, 1996; Weinlich et al., 1998). After leaving the epidermis, LCs encounter the basement membrane, where the collagen forms a dense meshwork that obstructs LC migration. In the dermis, collagen-dense connective tissue renders the movement of DCs difficult until they encounter a lymphatic vessel. LCs produce digestive enzymes such as metalloprotease 2 (MMP-2) and MMP-9 to facilitate passage through the basement membrane and the dermal extracellular matrix (ECM) (Ratzinger et al., 2002; Kobayashi, 1997).

The ECM functions not only in tissue scaffolding, but also in the regulation of cell migration, proliferation and differentiation. The role of the ECM in cancer metastases became evident when 2D and 3D systems were compared and the requirement of digestive enzymes to degrade the 3D network, allowing cell migration, was shown (Hotary et al., 2003). ECM is composed of structural proteins, proteoglycans, growth factors and matricellular proteins such as thrombospondin 1 (TSP1) and TSP2, osteopontin, tenascin-C and SPARC (secreted protein acidic and rich in cysteine).

SPARC, also known as osteonectin or BM-40, is a calcium-binding glycoprotein secreted by many cells types (Bradshaw and Sage, 2001). In vivo, SPARC is expressed during tissue remodeling, such as in cutaneous wound healing, bone formation, adipogenesis and angiogenesis, and its role is primarily regulatory rather than structural. Targeted disruption of the SPARC gene in mice results in early cataractogenesis (Gilmour et al., 1998; Norose et al., 1998), osteopenia (Delany et al., 2003) and curly tails (Bradshaw and Sage, 2001). Dermal ECM of SPARC-null mice has 50% less collagen deposition than does age-matched wild-type skin, a feature that favors wound healing by facilitating skin contraction (Bradshaw et al., 2002).

The observation that SPARC induces loss of focal adhesion and regulates the expression of MMPs (Tremble et al., 1993) and plasminogen-activator factor (Hasselaar et al., 1991) suggests a role for SPARC in modulating cell migration in vivo. This might depend either on SPARC produced by migrating cells or on structural SPARC, which forms part of basal membranes and ECM. In SPARC-null mice, while increased neutrophil and leukocyte infiltration occurs in bleomycin-induced peritonitis (Savani et al., 2000) and TPA-induced skin inflammation (Sangaletti et al., 2003), respectively, the mechanism underlying this effect has not been investigated yet. Similarly, the role of SPARC in tissue remodeling through its binding to collagen type IV in basal membrane, and to collagen type I in the dermis, has not been

linked directly to cell migration (Yan et al., 2003; Yan et al., 2002; Wewer et al., 1988). In transplanted mammary tumors we recently demonstrated that the lack of SPARC production prevents proper basal membrane assembly disrupting the stromal shield that protects the tumors from immune attack (Sangaletti et al., 2003). However, whether the aberrantly organized dermal ECM in SPARC-null mice could influence leukocyte migration and, in turn, systemic immune response has not been previously investigated. In this work we analyzed the involvement of SPARC, either produced by migrating cells or as part of tissue environment, in antigen-specific immune responses. To this end we (1) tested the in vivo migration of LCs and DCs in SPARC-null and SPARC-sufficient mice, as well as that of DCs from mice following injection into both null and sufficient host; (2) compared cutaneous contact hypersensitivity (CHS), delayed type hypersensitivity (DTH) and in vivo priming of CD4 transgenic T cells in SPARC-null and wild-type mice; and (3) discriminated between SPARC produced by migrating cells from that present in the tissue environment using bone marrow (BM) chimeras in which BM-derived cells, including LCs, were either from SPARC$^{-/-}$ or SPARC$^{+/+}$ donors. Our results describe a faster CHS and DTH in SPARC-null mice owing to enhanced DC migration and accelerated T-cell priming because of a less dense collagen and less structured ECM.

Materials and Methods

Mice
SPARC$^{-/-}$ KO mice, originally on a mixed 129SV/C57BL/6 background, were backcrossed for 12 generations with BALB/cAnNCrl (Charles River, Calco, Italy) to obtain congenic SPARC$^{-/-}$ mice as described (Sangaletti et al., 2003). Mice were bred and maintained at the Istituto Nazionale Tumori under standard conditions, according to institutional guidelines. BALB/cAnNCrl and (BALB/c × C57BL/6)F1 (hereafter, referred to as CB6F1) were purchased from Charles River. OVA-specific, MHC class II-restricted TCR transgenic mice DO11.10 were kindly provided by L. Bruno (Basel Institute of Immunology).

Skin organ culture
Ears removed from wt and SPARC$^{-/-}$ mice were soaked in ethanol, air-dried for 10 minutes and then separated along the dorsal-ventral axis. Dorsal halves were incubated, dermal side down, for 1 or 2 days at 37°C in 24-well tissue culture plates (Costar, Cambridge, MA) (one ear per well) in 1.5 ml of culture medium supplemented with 5 ng/ml of recombinant granulocyte-macrophage colony-stimulating factor (rGM-CSF) (Endogen, Woburn, MA). Cells that had emigrated into the medium were collected from the wells each day. LCs were identified and quantified by hemocytometry based on the typical veiled and hairy appearance of these cells, as well as by flow cytometry using specific antibodies (Abs). Cells from at least eight explants were pooled, fixed in 1% PFA solution for 10 minutes, permeabilized with 0.1% saponin solution and incubated with primary Abs or isotype-matched controls for 30 minutes at 4°C. After washing, cells were incubated with second-step reagents for 30 minutes at 4°C and re-washed before analysis.

Primary mAbs included the rat anti-mouse Langerin/CD207 (Valladeau et al., 2002) (clone 929F3, kindly provided by Sem Sealand, Schering-Plough, Dardilly, France), NLDC145 (Cedarlane, Homby, Ontario, Canada) and PE-conjugated I-A/I-E, clone M5/114.15.2 (BD-Bioscience). Second-step reagents included FITC-labeled and biotinylated goat anti-rat IgG and FITC-conjugated

streptavidin, all from DakoCytomation (Milano, Italy). Single- and two-color analysis was performed using a FACScalibur and dedicated Cell Quest software (both from Becton Dickinson).

Epidermal sheet preparation and immunostaining
The epidermis was separated from the dermis by placing dorsal ear-halves, dermal side down, in a 0.5 M ammonium thiocyanate for 30 minutes at 37°C (Ratzinger et al., 2002). Epidermal sheets were fixed in acetone and immunolabeled sequentially using the following antibodies: rat anti-mouse Langerin/CD207, rat anti-mouse I-A^d/I-E^d (clone 2G9) or rat anti-mouse I-A^b (clone AF6-120.1) (overnight at 4°C), and biotinylated goat anti-rat (1 hour at room temperature) and streptavidin-peroxidase (1 hour at room temperature). Peroxidase activity was visualized with 3'3'-diaminobenzidine (DAB, Sigma Immunochemicals). The density of LCs in epidermal sheets was assessed in 20 randomly selected fields using a 20× objective of a Nikon microscope (Nikon Instruments, Sesto Fiorentino, Italy) equipped with a Nikon digital camera (DXM1200) and analyzed using ACT1 software.

Contact hypersensitivity assay
The contact sensitizer 2,4-dinitro-1-fluorobenzene (DNFB) (Sigma Immunochemicals, Milano, Italy) was applied to each side of the right ears of naive mice (20 μl/side) at the subtoxic concentration of 0.5% in acetone-olive oil (4:1). Five days after sensitization, the dorsal side of the left ear was challenged with 20 μl of 0.2% DNFB in acetone-olive oil. Twenty-four and 48 hours after challenge, ear thickness was measured with a micrometer and compared with control mice, which received the challenge but not the priming (Phanuphak et al., 1974). Five independent experiments, with 7 mice/group, were carried out.

Immunization protocol for delayed-type hypersensitivity
Mice (7/group) were injected subcutaneously with 400 μg of OVA (grade V, Sigma) emulsified in CFA in the dorsal side of the right ear. Either 48 hours or 5-days later, mice were challenged with 200 μg of OVA in IFA into the dorsal side of the left ear. As controls, sensitized mice were challenged with medium alone.

Histology and immunostaining of skin and draining LN
For histological analysis, ear skin treated with or without DNFB was fixed in 10% neutral buffered formalin, embedded in paraffin, sectioned and stained with hematoxylin and eosin (H&E) or Masson's trichrome as described (Sangaletti et al., 2003).

For immunohistology, draining LN were collected 24 and 48 hours after DNFB priming, whereas the skins of sensitized mice were obtained 24 and 48 hours after DNFB challenge. Draining LNs and skin were embedded in optimal cutting compound (OCT), snap-frozen in liquid nitrogen and sectioned at 5 μm. Sections were subsequently fixed in acetone for 10 minutes, placed in 3% H$_2$O$_2$/MeOH solution for 5 minutes to block endogenous peroxidase activity, rinsed in PBS, blocked in 5% FCS for 20 minutes and immunostained with Langerin/CD207. After washing, sections were sequentially overlaid with biotinylated goat anti-rat IgG for 30 minutes and avidin-peroxidase complex for 30 minutes (Sigma). Antigen was revealed with DAB (Sigma) according to the manufacturer's instructions. Sections were counterstained with Mayer's hematoxylin, dehydrated in graded alcohol (70%, 95% and 100% ethanol) and mounted in BDH mounting medium (Merck Eurolabs, Milano, Italy). All immunolocalization experiments were repeated three times with multiple sections, including negative controls for determination of background staining using the appropriate isotype-matched control.

Latex migration

Mice under ketamine/xylazine anesthesia were injected into the dorsal side of both ears with 10^7 of yellow-green-latex (LX) microspheres (1 μm diameter) (Polyscience) as tracer. Since at the steady state, few DCs migrate to the draining LN, the same ears were painted with DNFB 30 minutes later to create an inflammatory environment. Eight and 24 hours after bead injection, cervical LNs were collected and cells were released by treatment with 1 mg/ml of collagenase D (Roche) for 20 minutes at 37°C. Cells were stained for MHC class II and CD11c expression. The entire cell population of draining LN was analyzed by cytofluorimetry and the absolute number of I-A^d/I-E^{d+} or CD11c$^+$-containing green-LX microspheres determined as described (Rotta et al., 2003).

In vitro loading of DCs with latex microspheres and mouse treatment

Murine DCs were generated from bone marrow (BM) of SPARC$^{+/+}$ mice and SPARC$^{-/-}$ mice. Briefly, BM was harvested by flushing femurs and tibias with medium. Cells were resuspended at 2×10^6 cells/ml in cRPMI-1640 (Gibco) supplemented with 5 ng/ml of rGM-CSF and 10 ng/ml of murine rIL4 (Endogen). On days 3 and 5 of culture, half of the medium was replaced with fresh medium containing GM-CSF and IL4. On day 6, loosely adherent cells were harvested by gentle pipetting and DCs were purified with CD11c MiniMacs columns according to the manufacturer's instructions (Miltenyi Biotec, Bologna, Italy). Phenotype of the purified CD11c$^+$ fraction was analyzed by flow cytometry using Abs to CD11c, B7.2, CD40, H-2K^d, I-A^d/I-E^d. DCs were incubated with green-LX- or red-LX-microspheres (1:100, DCs: microspheres) for 30 minutes at 37°C, and uptake of the LX-microspheres was determined by FACS analysis of CD11c-gated cells. 5×10^5 green-LX-loaded DCs from SPARC$^{+/+}$ and 5×10^5 red-LX-loaded DCs from SPARC$^{-/-}$ mice (or vice versa) were injected intradermally in the dorsal ear skin of anesthetized SPARC$^{+/+}$ or SPARC$^{-/-}$ mice (7 mice/group, 2 independent experiments). Mice were sacrificed 48 hours after injection and draining LN were collected and cells analyzed by FACS.

T-cell transfer and immunization

T cells were enriched from spleens of DO11.10 OVA transgenic mice by nylon wool separation. CD8 and B220 cells were eliminated by magnetic beads coated with α-CD8 and α-B220 mAb. The negative fraction contained up to 90% CD4$^+$ T cells. To obtain naive CD4$^+$CD25$^-$ cells, CD4$^+$CD25$^+$ cells were eliminated by magnetic bead separation using anti-CD25PE (PC61; Caltag) followed by magnetic beads-anti-PE (Miltenyi Biotec, Italy). The negative fraction of this separation contained up to 95% clonotype-specific CD4$^+$CD25$^-$ cells. CD4$^+$CD25$^-$ cells were labeled with 1 μM carboxy-fluorescein diacetate succinimidyl ester (CFSE; Molecular Probes) for 15 minutes at 37°C before transferring 3×10^6 cells into recipient mice by tail vein injection. OVA protein (Sigma-Aldrich) was emulsified in CFA (Sigma-Aldrich) and 400 μg was administered intradermally in the dorsal side of the ear pinna. LN draining the site of injection were stained with clonotype-specific mAb KJ1.26-PE (Caltag) and analyzed by FACS for decreased CFSE staining as a function of cell proliferation. The number of transgenic T cells in each LN was calculated as percentage of KJ1.26$^+$/CFSE$^+$ cells among the total cell number.

Chemotaxis assay

BM DCs obtained from SPARC$^{+/+}$ and SPARC$^{-/-}$ mice were tested in vitro for migration in response to CCL20 (MIP-3α). Briefly, triplicate assays were carried out in 96-well microchemotaxis chambers (Neuro Probe, Cabin John, MA) with a 5 μm pore polycarbonate membrane (Costar) separating cells from the medium containing different amounts of MIP-3α (Peprotec). DCs (2×10^6/ml) were allowed to migrate for 2 hours in DMEM medium containing 0.1% BSA. As a control, replicate samples were pretreated with 200 ng/ml pertussin toxin (Sigma, cat. no. P708) for 1 hour at 37°C. The membrane was removed and stained using the Diff Quick kit. Migrated cells were counted under a microscope (40× objective). Migration index was calculated as the number of cells migrated in the presence of recombinant chemokine divided by the number in medium alone.

Bone marrow transplantation (BMT)

SPARC$^{+/+}$ and SPARC$^{-/-}$>CB6F1 as well as CB6F1>SPARC$^{+/+}$ and CB6F1>SPARC$^{-/-}$ chimeras were obtained as described (Sangaletti et al., 2003). Engraftment was verified 8 weeks after BMT by staining peripheral blood mononuclear cells (PBMCs) obtained from the retro-orbital sinus with FITC-conjugated mouse anti-mouse H-2K^b and PE-conjugated mouse anti-mouse H-2K^d, as well as isotype control FITC- and PE-conjugated mouse IgG2a, and then analyzing by cytofluorimetry.

UV irradiation

The ear skin of BM chimeras and of control SPARC$^{+/+}$ and SPARC$^{-/-}$ mice was exposed to UV radiation (wavelength, 254 nm; voltage, 8W; source distance, 38 cm from the target) twice for 30 minutes each time with a 4 hour interval using a UV lamp (Ultra-violet Products, Cambridge, UK). Three weeks later, UV-irradiated and non-irradiated control mice were painted with 0.5% DNFB to induce CHS. The H-2 haplotype of remaining host or recruited donor LCs was determined by staining epidermal sheets of chimeric mice with anti-MHC-II antibody 1 and 3 weeks after UV irradiation, as described above.

Statistical analyses

Data are expressed as mean±s.d. Statistical analyses were performed using the Mann-Whitney t-test. Differences were considered significant at $P\leq0.05$.

Results

SPARC$^{-/-}$ mice show exaggerated CHS in response to DNFB

To test whether the extracellular matrix protein SPARC influences the antigen-specific immune response, we tested CHS in response to DNFB in SPARC$^{+/+}$ and SPARC$^{-/-}$ mice.

As shown in Fig. 1A, ear thickness of mice sensitized by applying DNFB to the dorsal side of the right ear and challenged 5 days later with DNFB on the left ear was significantly higher ($P<0.01$) in SPARC$^{-/-}$ mice than in SPARC$^{+/+}$ mice at both 24 and 48 hours after challenge. Histological analysis and immunohistochemistry of swollen ears revealed greater edema and a higher number of neutrophils and macrophages in tissues from SPARC$^{-/-}$ than those from SPARC $^{+/+}$ mice (Fig. 1B and data not shown).

Greater numbers of epidermal LCs migrate to draining LNs upon DNFB sensitization in SPARC$^{-/-}$ mice than in wild-type mice

Immunostaining analysis of epidermal sheets from ear pinnae of SPARC$^{-/-}$ and wild-type mice revealed essentially the same number of Langerin/CD207$^+$ cells (53.8±4.4 per field vs 50.9±3.8 per field, respectively) and the same staining intensity (Fig. 2A), indicating that the enhanced CHS observed in
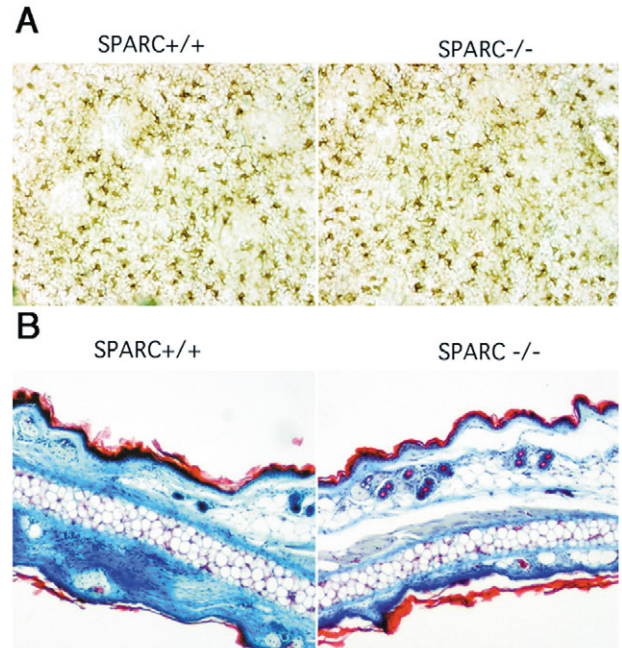
A

B

SPARC +/+   SPARC-/-
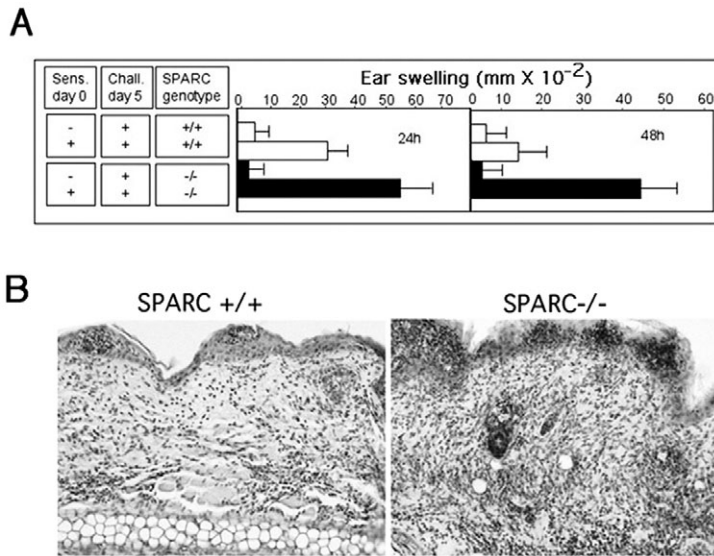
Fig. 1. Enhanced CHS in SPARC-knockout mice. SPARC^{+/+} and SPARC^{−/−} mice were sensitized with DNFB on the dorsal side of the right ear on day 0. Five days later, mice were challenged on the left ear. Control mice from the two strains were treated only with the challenge dose of DNFB. Panel A shows ear swelling measurements (mean±s.d.) at 24 and 48 hours after challenge for each group of mice. Mean values were significantly different at both time points ($P<0.001$). Results are representative of five independent experiments. Panel B shows the inflammatory response in sections of the challenged ear of SPARC^{+/+} and SPARC^{−/−} mice. Tissues were harvested 24 hours after DNFB challenge, fixed in 10% neutral buffered formalin and sections stained with hematoxylin and eosin. Owing to extensive swelling, only a portion of the SPARC^{−/−} section is shown (cartilage is below the cut line of the figure and was omitted to ensure a magnification matching that of the control panel). Inflammatory infiltrate appears to be more abundant in the SPARC^{−/−} section.

A

SPARC+/+   SPARC-/-

B

SPARC+/+   SPARC -/-

Fig. 2. The same numbers of Langerhans cells (Langerin/CD207^{+}) but different collagen content characterize the ear skin of SPARC^{+/+} and SPARC^{−/−} mice. (A) The distribution of Langerin/CD207^{+} cells in the epidermal sheet from untreated SPARC^{+/+} and SPARC^{−/−} mice is very similar. Cell counting and morphometry revealed essentially the same numbers of LCs in the epidermal sheet of the two strains (SPARC[+/+]=50.9±7.5 and SPARC[−/−]=53.8±4.4 in 10 randomly chosen fields, n=5). (B) Total ear collagen content and distribution are shown in cross-sections of the middle auricles by trichromic stain. SPARC^{+/+} ear pinna is characterized by a greater amount of collagen on both sides of the cartilage; increased thickness of the internal face of auricles and minor evidence of external auricle subcutaneous fat and muscle structures are seen compared with SPARC^{−/−} ear pinnae.

SPARC^{−/−} mice is not due to a different density of LCs in the sensitized skin.

Because the skin of SPARC^{−/−} mice has less dense collagen than that of wild-type mice (Fig. 2B), we monitored Langerin/CD207^{+} cells in the draining LN to determine whether the enhanced CHS in SPARC^{−/−} mice reflects more efficient priming as a result of enhanced LC migration to draining nodes; in fact, a significantly higher number of LCs were detected in LNs from SPARC^{−/−} mice than those from wild-type mice at both 24 and 48 hours after sensitization (Fig. 3A,B).

LNs from SPARC^{−/−} mice have greater numbers of microsphere-loaded cells

To further assess whether the absence of SPARC favors DC migration, we monitored the migration of DCs loaded in vivo with green-latex (LX) microspheres. SPARC^{+/+} and SPARC^{−/−} mice were injected with 10^7 LX microspheres into the dorsal side of the right ear, which was painted with DNFB 30 minutes later. Draining LNs were collected after 8 and 24 hours, and cells were immunolabeled with PE-conjugated anti-I-A[d]/I-E[d] for two-color FACS analysis. As shown in Fig. 4A, the frequency of I-A[d]/I-E[d+]/LX-loaded DCs in the draining LN

was significantly higher in SPARC^{−/−} mice than in SPARC^{+/+} mice at both time points. Morphologically, LX-loaded cells appeared typically hairy and veiled (Fig. 4B). DC migration to the draining LN was also associated with increased LN cellularity and swelling (Fig. 4C and data not shown), consistent with a recent report (Martin-Fontecha et al., 2003). To control for the possibility that the microspheres observed had reached the LN freely or were taken up by DCs present in draining LN rather than by migrating DCs, green and red microspheres were injected in adjacent but non-overlapping sites drained by the same LN; microsphere-loaded DCs collected from draining LNs after 8 and 24 hours were either green or red but never double-stained (supplementary material Fig. S1), demonstrating that beads do not reach draining LNs unless engulfed by DCs, as previously reported (Randolph et al., 1999).

The SPARC genotype of DCs does not influence their migration

To confirm the enhanced migration of DCs in SPARC^{−/−} mice even in the absence of DNFB-induced inflammation, and to
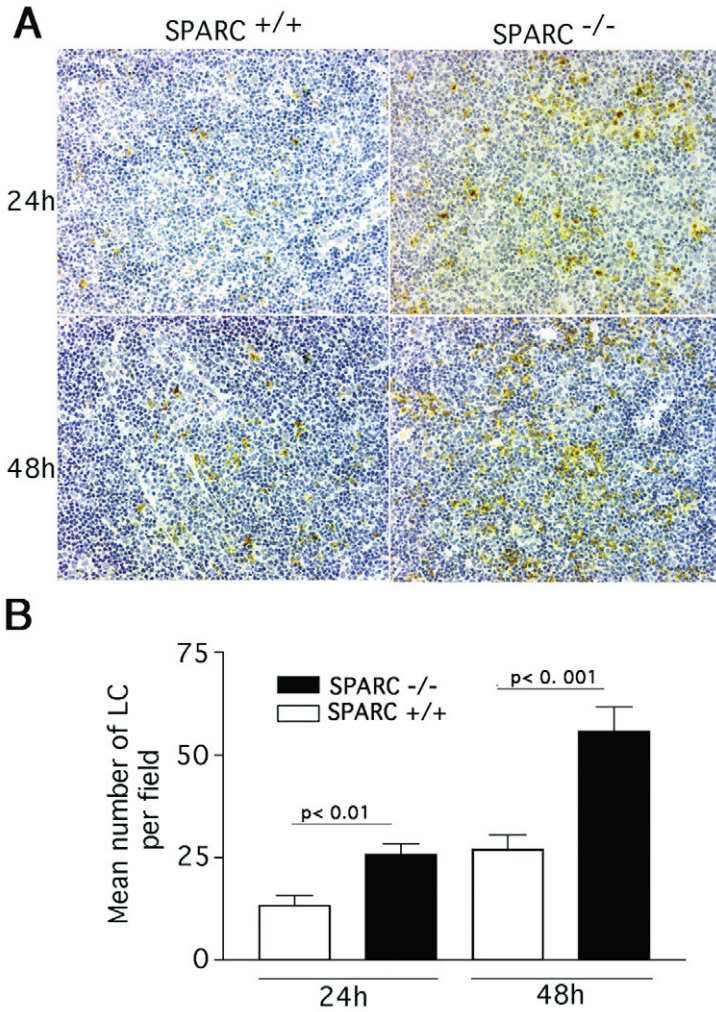
Fig. 3. Distribution of Langerhans/CD207^{+} cells into the draining LN of SPARC^{+/+} and SPARC^{−/−} mice after DNFB sensitization. Draining LNs were removed 24 and 48 hours after sensitization, sectioned and stained with mAb to Langerin/CD207. Langerin/CD207^{+} cells were counted under a microscope with a 20× objective. Panel A shows representative Langerin staining of draining LN from SPARC^{+/+} and SPARC^{−/−} mice collected 24 and 48 hours after DNFB painting. Panel B shows the number (mean±s.d.) of Langerin/CD207^{+} cells counted in 10 randomly chosen fields from six independent preparations for each SPARC^{+/+} and SPARC^{−/−} experimental group.

evaluate the role of DC-produced SPARC in migration we pre-loaded in vitro BM-derived DCs from SPARC^{+/+} and SPARC^{−/−} mice with green- or red-LX microspheres, respectively (or vice versa), before co-injecting them (5×10^5 each) intradermally into the ear dorsal side of SPARC^{+/+} or SPARC^{−/−} mice. Draining LN were collected after 48 hours and cells were analyzed by FACS. In accordance with the previous experiment, the absolute number of LX-microsphere-loaded DCs in the draining LN was higher when the cells were injected into SPARC^{−/−} mice than when injected into SPARC^{+/+} mice (Fig. 5A), regardless of the DC SPARC genotype (Fig. 5A,B and data not shown). The difference in the extent of DC migration was not due to different intrinsic migratory capacities of the DCs from SPARC^{+/+} and SPARC^{−/−} mice, since in vitro analysis of BM-derived DCs revealed no difference in migration of the DCs from the two strains in response to various amounts of MIP-3α (supplementary material Fig. S2). Moreover, DCs from both strains showed a similar phenotype, maturation and cytokine production pattern in response to bacterial stimuli (data not shown).
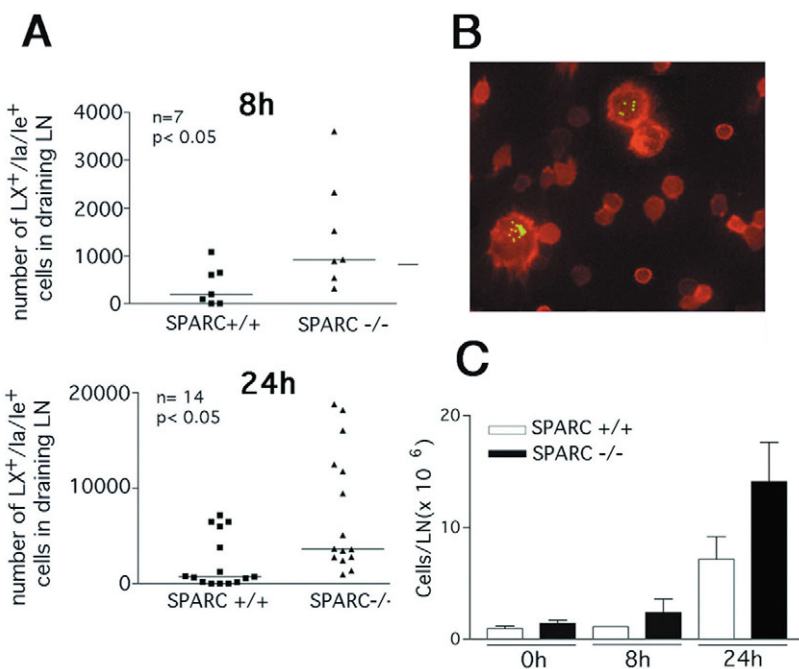
Impact of enhanced DC migration on T-cell priming

The sensitization phase of the CHS response to a hapten depends on T-cell priming by antigen-loaded DCs, in particular, LCs. Typically, the efferent phase can be induced within 5 days of

Fig. 4. Migration of LX-bearing cells in the draining LN and consequent increase in LN cellularity. (A) SPARC^{+/+} and SPARC^{−/−} were injected with 10^7 green-LX-microspheres in the dorsal side of the right ear, which was painted with DNFB 30 minutes later. Draining LNs were collected after 8 and 24 hours and cells were immunolabeled with PE-conjugated anti-I-A[d]/I-E[d] for two-color FACS analysis. A higher number of green-LX-loaded/ I-A[d]/I-E[d]+ cells were found in draining LNs from SPARC^{−/−} than from SPARC^{+/+} mice at both 8 and 24 hours after treatment. (B) Morphology of green-LX-loaded/ I-A[d]/I-E[d]+ cells in the draining LN reveals the typical hairy and veiled appearance of DCs. (C) Total cell number in the draining LN of treated mice. Migration of green-LX-loaded/ I-A[d]/I-E[d]+ cells in the draining LN is associated with increased LN cellularity which is more extensive in SPARC^{−/−} mice.

Fig. 5. Migration of BM DCs does not depend on their SPARC genotype. We pre-loaded in vitro BMDCs from SPARC$^{+/+}$ and SPARC$^{-/-}$ mice with green- or red-LX microspheres, respectively (or vice versa), before co-injecting them (5×10^5 each) intradermally into the ear dorsal side of SPARC$^{+/+}$ or SPARC$^{-/-}$ mice. Draining LN were collected after 48 hours and analyzed by FACS. (A) An example of SPARC$^{+/+}$ green-LX- and SPARC$^{-/-}$ red-LX-loaded DCs in draining LN from SPARC$^{+/+}$ mice. (B) Cumulative data of all tested combinations. A higher number of green- or red-LX-loaded DCs was found in draining LNs of SPARC$^{-/-}$ mice, regardless of the SPARC genotype of the LX-loaded DCs. Each bar represents the mean value of 14 LNs analyzed (7 mice/group).
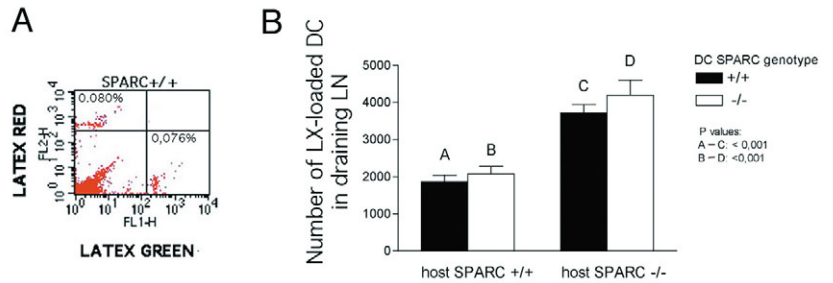
sensitization. To test whether the faster migration of DCs in the absence of SPARC accelerates the time of priming, we challenged sensitized and control naive SPARC$^{+/+}$ and SPARC$^{-/-}$ mice with DNFB starting 48 hours after sensitization and every other day until day 5; at every time point, ear swelling of SPARC$^{-/-}$ mice was significantly greater than that of SPARC$^{+/+}$ mice (Fig. 6A). In addition, only SPARC-null mice showed a difference from non-sensitized mice in swelling at 24 hours after sensitization (not shown).

As alternative assay to test accelerated priming, we performed DTH in response to ovalbumin sensitization and challenged mice after 48 hours, which is 3 days earlier than the standard challenge time in this type of experiment. As shown in Fig. 6B, ears of SPARC$^{-/-}$ but not SPARC$^{+/+}$ mice swollen.

In addition, SPARC$^{-/-}$ and SPARC$^{+/+}$ mice were injected i.v. with OVA-specific transgenic T cells (from DO11.10 mice) immunolabeled with carboxy-fluorescein diacetate succinimidyl ester (CFSE), further injected with OVA protein in the ear pinna, and the draining LNs were collected 36 and 48 hours later for analysis of dye dilution as a function of cell divisions. At the earliest time point (36 hours after immunization), 62% and 35% of transgenic T cells were proliferating in SPARC$^{-/-}$ and SPARC$^{+/+}$, respectively (Fig. 6C), indicating accelerated priming of transgenic T cells in SPARC$^{-/-}$ mice. Moreover, the absolute number of transgenic T cells, and therefore of primed T cells, was higher in LNs from SPARC$^{-/-}$ than SPARC$^{+/+}$ mice (Table 1). Together, the results support the conclusion that OVA-loaded DCs arrive earlier and in larger numbers into the draining LNs of SPARC$^{-/-}$ compared with LNs of SPARC$^{+/+}$ mice.

Emigration of cutaneous DCs from skin explants

Skin explant is a well studied and characterized method to directly follow LC migration (Larsen et al., 1990); moreover, it shares similarities with CHS in terms of kinetics and pathway of DC migration (Weinlich et al., 1998). We prepared skin explants from SPARC$^{+/+}$ and SPARC$^{-/-}$ mice accordingly. The dorsal halves of the ear skins were cultured in 24-well tissue culture plates for 24 and 48 hours in the presence of recombinant granulocyte-macrophage colony-stimulating factor (rGM-CSF), and cells emigrating into the culture

Fig. 6. Effect of DC migration on T-cell priming. Panel A shows the accelerated CHS occurring in SPARC$^{-/-}$ mice. DNFB-sensitized SPARC$^{+/+}$ and SPARC$^{-/-}$ mice were challenged with DNFB starting 48 hours after sensitization and every other day until day 5. Ear swelling was measured 24 hours after challenge. At every time point, ear swelling was significantly higher ($P<0.05$) in SPARC$^{-/-}$ than in SPARC$^{+/+}$ mice. Panel B shows DTH elicited in SPARC$^{-/-}$ but not SPARC$^{+/+}$ challenged mice 48 hours after OVA sensitization. Panel C shows the effect of DC migration on priming of OVA-specific transgenic T cells. CFSE-labeled KJ$^+$CD4$^+$CD25$^-$ cells were adoptively transferred into SPARC$^{+/+}$ and SPARC$^{-/-}$ mice. Mice were immunized 8 hours later by injection of OVA protein into the ear pinna. Draining LNs were isolated at the indicated time points after immunization and stained with KJ-126-PE Ab. the histogram show the analysis from a representative mouse at each time point for SPARC$^{+/+}$ and SPARC$^{-/-}$ groups. See Table 1 for quantitative data analysis. M1 and M2 indicate non-divided and divided cells, respectively.
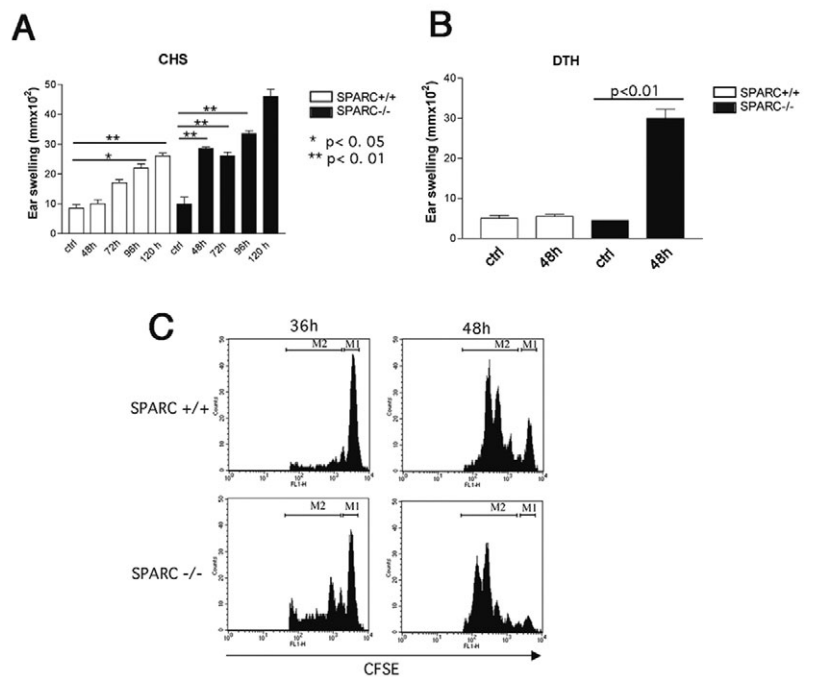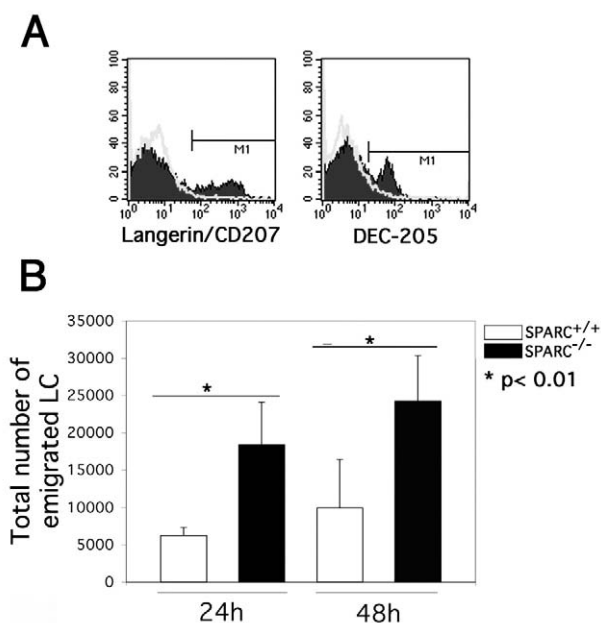
Table 1. Proliferation of clonogenic KJ+ CD4+ T cell in response to OVA immunization in SPARC+/+ and SPARC−/− mice

	% of KJ+CFSE+ cells divided or not at 36 and 48 hours				Total number of KJ+CFSE+ cells ($\times 10^3$)			
	SPARC+/+	SPARC−/−	SPARC+/+	SPARC−/−	SPARC+/+	SPARC−/−	SPARC+/+	SPARC−/−
	36 hours		48 hours		36 hours		48 hours	
M1	60±13	36±3*	14±2	7±3†	113±20	153±15†	254±30	590±73*
M2	35±12	62±12*	81±7	89±8†				

The table summarizes data from Fig. 6C. For each time point eight mice per group were analyzed. Statistical analysis was performed using Student's *t*-test; (*$P<0.001$ or †$P<0.05$).
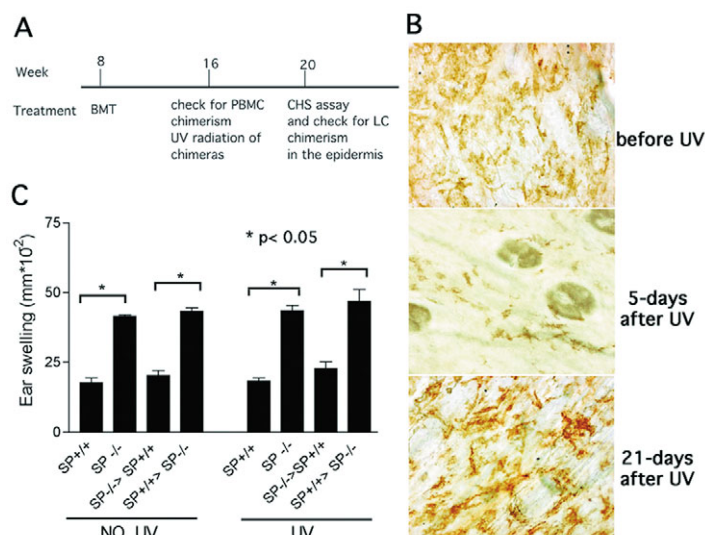
medium were evaluated. At least eight explants were pooled for each experiment. DCs were readily identified by their veiled and hairy appearance, and further characterized by flow cytometry using mAbs to DEC-205 and Langerin/CD207 (Fig. 7A). Of the emigrated cells collected at 24 and 48 hours, 19 and 23% were LCs, respectively (Langerin/CD207 stained), regardless of their SPARC genotype. However, the real number of LCs obtained from the ear skin, calculated as the total number of collected cells multiplied by the fraction of Langerin/CD207-stained cells, was significantly higher in SPARC−/− mice than in SPARC+/+ mice (Fig. 7B).

Enhanced CHS response in SPARC−/− mice does not depend on SPARC produced by BM-derived cells

To confirm the critical role of tissue environment in determining the in vivo leukocyte migration during Ag-specific CHS, we transplanted SPARC−/− mice with BM from wild-type (CB6) mice and vice versa to obtain chimeric mice expressing or not expressing SPARC in cells derived from their BM compartment (Fig. 8A). To ensure the donor origin of skin LCs, chimeras were UV-irradiated 8 weeks after BM transplantation to allow LC renewal from donor BM, in accordance with previous studies (Merad et al., 2002) (Fig. 8B). Three weeks later, UV-irradiated and non-irradiated mice were sensitized with DNFB to induce CHS. Ear swelling measured at 24 hours after challenge in SPARC+/+>SPARC−/− chimeras was identical

Fig. 7. Migration of Langerhans cells from skin explants. Ear skins (dorsal halves, cartilage-free) obtained from SPARC+/+ and SPARC−/− mice were cultured in 24-well tissue culture plates (one ear half per well) in the presence of rGM-CSF. (A) Cells that emigrated into the culture medium, were characterized by FACS with monoclonal antibody to Langerin/CD207 and DEC-205 as shown for SPARC+/+ explants as an example. (B) The mean number of Langerhans cells obtained from the ear skin of SPARC−/− mice, was significantly higher than that obtained from SPARC+/+ mice both at 24 and 48 hours of culture. The mean number of Langerhans cells was calculated as total number of collected cells multiplied by the fraction of Langerin/CD207+ stained cells. Results are representative of three independent experiments.

Fig. 8. CHS in chimeric mice depends on environmental SPARC. (A) SPARC+/+>SPARC−/− chimeric mice expressing SPARC only in their BM compartment and reciprocal SPARC−/−>SPARC+/+ chimeras were obtained by using, respectively, (CB6)F1 mice as donor or recipient in BM transplantation experiments. To ensure that LCs were of donor origin, chimeras were UV-irradiated 8 weeks later to allow LC renewal from BM precursors. Three weeks after radiation, chimeric and control mice (UV-irradiated or not) were tested for CHS. (B) Immunostaining of MHC-II haplotype in the epidermal sheet of SPARC+/+>SPARC−/− chimera before and after UV-irradiation at the indicated time points. (C) The degree of CHS was dependent on the host rather than donor SPARC genotype, with greater CHS in SPARC+/+>SPARC−/− chimeras, which did not differ from SPARC−/− control mice. No differences in ear swelling degree were detected in UV-irradiated and non-irradiated mice after replenishment of LCs from BM precursors, further confirming the role of environmental SPARC.

to that of SPARC$^{-/-}$ mice and ear swelling of SPARC$^{-/-}$>SPARC$^{+/+}$ chimeras did not differ from that of SPARC$^{+/+}$ mice, regardless of whether LCs were of SPARC$^{+/+}$ or SPARC$^{-/-}$ genotype (Fig. 8C). These results suggest that environmental SPARC rather than SPARC produced by migrating cells underlies the different extent of CHS.

Discussion

LC/DC migration is critical for T-cell priming. In the case of local elicitation of CHS, LCs capture and process epicutaneous Ag and migrate to the regional LN to present Ag to naive T cells. LC migration is known to be regulated by cytokines such as TNFα and IL-1β (Enk and Katz, 1992; Stoitzner et al., 1999) and to involve adhesion molecules such as I-CAM (Ma et al., 1994), E-cadherin (Tang et al., 1993; Schwarzenberger and Udey, 1996; Jakob and Udey, 1998), integrin-α6 (Price et al., 1997) and CD44 (Weiss et al., 1997). Recently, LCs were shown to create a path to the draining LN by digesting collagen in connective tissues, basement membranes and dermal extracellular matrix by means of MMP-2 and MMP-9 (Kobayashi, 1997; Ratzinger et al., 2002).

As for other matricellular proteins, SPARC expression is tightly regulated during development and tissue repair. SPARC is increased in response to skin injury and its absence is associated with a decreased deposition of collagen and with a delayed production of extracellular matrix proteins in the injured skin (Bradshaw et al., 2002). Here, we show that matricellular SPARC also contributes to antigen-specific immune responses by conditioning DC migration.

Because inflammatory cytokines promote DC migration by modulating both the chemokine receptor on these cells and the adhesion molecules of nearby tissues, it was important to determine whether LCs migrate faster in SPARC-null mice even in the absence of inflammatory stimuli. Experiments in which DCs were pre-loaded in vitro with fluorescent latex microspheres and injected in the ear skin of SPARC-null mice without any additional inflammatory stimuli revealed a significant increase in fluorescent DCs migrating to draining LN compared with those in SPARC-intact counterparts. Moreover, ear skin explants that directly show LC migration, from epidermis through the dermis into the culture medium containing rGM-CSF (Larsen et al., 1990; Weinlich et al., 1998) suggested that the increased emigration of LCs from the ears of SPARC$^{-/-}$ mice was related to their facilitated crossing of the dermal ECM because of its reduced collagen density. Indeed LCs require proteolysis to traverse basement membrane and dermis (Ratzinger et al., 2002). Although LCs can produce SPARC (not shown), our results point to environmental rather that cell-produced SPARC as a regulator of leukocyte migration.

LCs also migrate faster in SPARC-null than in wild-type mice in the presence of inflammatory stimuli, with the effector phase of CHS in SPARC$^{-/-}$ mice induced 48 hours after skin sensitization, whereas at least 72 hours was required to detect a slight swelling and 96 hours to reach statistical significance in BALB/c mice. Accordingly, when sensitized ears were removed as early as 8 hours, SPARC$^{-/-}$ mice still responded to challenge, suggesting that LCs had already migrated to draining LN (supplementary material Fig. S3). In addition to a more rapid priming, CHS is enhanced in SPARC$^{-/-}$ mice probably because of extensive recruitment of neutrophils and macrophages associated with pronounced edema and swelling. Thus, neutrophil infiltration at the site of challenge is required for CD8^{+} T-cell recruitment and elicitation of CHS (Dilulio et al., 1999), a process also described in immune-mediated tumor rejection (Colombo et al., 1992). Moreover, the greater edema and the massive neutrophil infiltration delays the remodeling of blood vessels necessary to normalize the inflamed tissue, thus explaining the persistent swelling observed up to 72 hours after challenge in SPARC$^{-/-}$ mice (not shown). Note that IL-10, which is mainly responsible for ending the CHS reaction (Berg et al., 1995), is normally produced in SPARC-null mice as revealed by immunohistochemistry (our unpublished results). Neutrophil accumulation in SPARC$^{-/-}$ mice has been associated with acute pulmonary inflammation and thioglycollate-induced peritonitis (Savani et al., 2000), suggesting a role for SPARC in regulating the inflammatory response.

We recently demonstrated that the absence of SPARC is associated with a defect in collagen type IV deposition in newly formed basement membrane-like structures (Sangaletti et al., 2003) that characterize lobular mammary carcinoma. In general, the absence of SPARC has been extensively associated with a defect in collagen deposition during tissue remodeling and also in normal skin (Puolakkainen et al., 2003), a defect that we have confirmed in mouse ear pinnae. These common defects led to our hypothesis that in the absence of SPARC, newly formed or remodeled matrix is less structured and therefore easier to degrade and more accessible to leukocyte migration. As part of the ECM, SPARC might control the inflammatory response by regulating the deposition of structural components such as collagens which, depending on the tissue type, are predominantly type I or type IV, to create a barrier against leukocyte infiltration. In addition, SPARC might control the availability of inflammatory cytokines, as shown for PDGF (Raines et al., 1992) and FGF (Hasselaar and Sage, 1992).

Little is known about the role of ECM and matricellular proteins in influencing leukocyte migration, skin injury or the inflammatory response. TSP2, a matricellular protein that shares some functions with SPARC with respect to collagen fibrillogenesis (Puolakkainen et al., 2003), is also involved in CHS; TSP2-null mice show an increased and prolonged CHS in response to oxazolone due to exaggerated inflammation and angiogenesis (Lange-Asschenfeldt et al., 2002). Tenascin-C is another matricellular protein with anti-adhesive properties and with a pattern of expression similar to that of SPARC. Tenascin-C-null mice showed increased DNFB-induced dermatitis compared with wild-type mice (Koyama et al., 1998). Unlike SPARC-null mice, osteopontin (OPN)-deficient mice show reduced CHS, consistent with the chemotactic activity of OPN in guiding DCs from the skin to lymphatic tissue (Weiss et al., 2001). Since SPARC is produced by leukocytes, including DCs (our unpublished results), it was important to distinguish between leukocyte- and host-derived SPARC in DC migration. Fluorescent latex microsphere-loaded DCs from SPARC$^{+/+}$ and SPARC$^{-/-}$ mice migrated similarly in the SPARC$^{+/+}$ host, whereas both migrated faster and to the same extent in SPARC$^{-/-}$ recipients. Moreover, BM transplantation clearly showed that environmental SPARC rather than leukocyte-produced SPARC determines the extent

of CHS. This finding appears to contrast with our previous report showing that SPARC produced by BM-derived cells is instrumental in building tumor-associated stroma (Sangaletti et al., 2003), but it may simply distinguish the reversible ECM rearrangement associated with inflammation from the progressive and permanent ECM reshuffling that accompanies tumor outgrowth. Alternatively, it may be that different BM-derived cell types localize in tumor versus inflamed tissue. Because of LC resistance to γ-irradiation (Allan et al., 2003; Merad et al., 2002), the skin of CB6>SPARC$^{-/-}$ and SPARC$^{-/-}$>CB6 BM chimeras were UV-irradiated to ensure the replacement of LCs with those of donor origin (Merad et al., 2002). Even in this setting, LC migration was shown to depend on the presence of SPARC in the embedding, surrounding tissue rather than on their own produced SPARC, as confirmed by our in vitro data showing that BM-derived DCs migrate equally in response to CCL20 regardless of their SPARC genotype.

Accelerated priming because of faster DC migration in the absence of SPARC is a general phenomenon that extends to the specific DTH reaction, which can be mounted in 2 days in SPARC$^{-/-}$ mice versus 5 days in SPARC$^{+/+}$ mice, as well as to the priming of naive DO11.10 TCR-transgenic T cells transferred into SPARC$^{+/+}$ and SPARC$^{-/-}$ mice and immunized with OVA protein. Although impaired or accelerated in vivo DC migration has been described to occur because of altered DC molecules such as MMP9 (Kobayashi et al., 1999) or Jam-a (Cera et al., 2004), our studies provide the first demonstration of host-determined obstacles to DC migration.

In conclusion, we provide evidence that environmental SPARC, by determining the tightness of the ECM, influences the migration of DCs to the draining LN and therefore the timing and extent of T-cell priming. Considering the extensive edema associated with CHS in SPARC-null mice, the results also raise the possibility that SPARC has anti-inflammatory properties, probably exerted through ECM rearrangement.

References

Allan, R. S., Smith, C. M., Belz, G. T., van Lint, A. L., Wakim, L. M., Heath, W. R. and Carbone, F. R. (2003). Epidermal viral immunity induced by CD8alpha+ dendritic cells but not by Langerhans cells. *Science* **301**, 1925-1928.

Austyn, J. M. (1996). New insights into the mobilization and phagocytic activity of dendritic cells. *J. Exp. Med.* **183**, 1287-1292.

Berg, D. J., Leach, M. W., Kuhn, R., Rajewsky, K., Muller, W., Davidson, N. J. and Rennick, D. (1995). Interleukin 10 but not interleukin 4 is a natural suppressant of cutaneous inflammatory responses. *J. Exp. Med.* **182**, 99-108.

Bradshaw, A. D. and Sage, E. H. (2001). SPARC, a matricellular protein that functions in cellular differentiation and tissue response to injury. *J. Clin. Invest.* **107**, 1049-1054.

Bradshaw, A. D., Reed, M. J. and Sage, E. H. (2002). SPARC-null mice exhibit accelerated cutaneous wound closure. *J. Histochem. Cytochem.* **50**, 1-10.

Cera, M. R., Del Prete, A., Vecchi, A., Corada, M., Martin-Padura, I., Motoike, T., Tonetti, P., Bazzoni, G., Vermi, W., Gentili, F. et al. (2004). Increased DC trafficking to lymph nodes and contact hypersensitivity in junctional adhesion molecule-A-deficient mice. *J. Clin. Invest.* **114**, 729-738.

Colombo, M. P., Modesti, A., Parmiani, G. and Forni, G. (1992). Local cytokine availability elicits tumor rejection and systemic immunity through granulocyte-T-lymphocyte cross-talk. *Cancer Res.* **52**, 4853-4857.

Delany, A. M., Kalajzic, I., Bradshaw, A. D., Sage, E. H. and Canalis, E. (2003). Osteonectin-null mutation compromises osteoblast formation, maturation, and survival. *Endocrinology* **144**, 2588-2596.

Dilulio, N. A., Engeman, T., Armstrong, D., Tannenbaum, C., Hamilton, T. A. and Fairchild, R. L. (1999). Groalpha-mediated recruitment of neutrophils is required for elicitation of contact hypersensitivity. *Eur. J. Immunol.* **29**, 3485-3495.

Enk, A. H. and Katz, S. I. (1992). Early molecular events in the induction phase of contact sensitivity. *Proc. Natl. Acad. Sci. USA* **89**, 1398-1402.

Gilmour, D. T., Lyon, G. J., Carlton, M. B., Sanes, J. R., Cunningham, J. M., Anderson, J. R., Hogan, B. L., Evans, M. J. and Colledge, W. H. (1998). Mice deficient for the secreted glycoprotein SPARC/osteonectin/BM40 develop normally but show severe age-onset cataract formation and disruption of the lens. *EMBO J.* **17**, 1860-1870.

Hasselaar, P. and Sage, E. H. (1992). SPARC antagonizes the effect of basic fibroblast growth factor on the migration of bovine aortic endothelial cells. *J. Cell Biochem.* **49**, 272-283.

Hasselaar, P., Loskutoff, D. J., Sawdey, M. and Sage, E. H. (1991). SPARC induces the expression of type 1 plasminogen activator inhibitor in cultured bovine aortic endothelial cells. *J. Biol. Chem.* **266**, 13178-13184.

Hotary, K. B., Allen, E. D., Brooks, P. C., Datta, N. S., Long, M. W. and Weiss, S. J. (2003). Membrane type I matrix metalloproteinase usurps tumor growth control imposed by the three-dimensional extracellular matrix. *Cell* **114**, 33-45.

Jakob, T. and Udey, M. C. (1998). Regulation of E-cadherin-mediated adhesion in Langerhans cell-like dendritic cells by inflammatory mediators that mobilize Langerhans cells in vivo. *J. Immunol.* **160**, 4067-4073.

Kobayashi, Y. (1997). Langerhans' cells produce type IV collagenase (MMP-9) following epicutaneous stimulation with haptens. *Immunology* **90**, 496-501.

Kobayashi, Y., Matsumoto, M., Kotani, M. and Makino, T. (1999). Possible involvement of matrix metalloproteinase-9 in Langerhans cell migration and maturation. *J. Immunol.* **163**, 5989-5993.

Koyama, Y., Kusubata, M., Yoshiki, A., Hiraiwa, N., Ohashi, T., Irie, S. and Kusakabe, M. (1998). Effect of tenascin-C deficiency on chemically induced dermatitis in the mouse. *J. Invest. Dermatol.* **111**, 930-935.

Lange-Asschenfeldt, B., Weninger, W., Velasco, P., Kyriakides, T. R., von Andrian, U. H., Bornstein, P. and Detmar, M. (2002). Increased and prolonged inflammation and angiogenesis in delayed-type hypersensitivity reactions elicited in the skin of thrombospondin-2-deficient mice. *Blood* **99**, 538-545.

Larsen, C. P., Steinman, R. M., Witmer-Pack, M., Hankins, D. F., Morris, P. J. and Austyn, J. M. (1990). Migration and maturation of Langerhans cells in skin transplants and explants. *J. Exp. Med.* **172**, 1483-1493.

Ma, J., Wang, J. H., Guo, Y. J., Sy, M. S. and Bigby, M. (1994). In vivo treatment with anti-ICAM-1 and anti-LFA-1 antibodies inhibits contact sensitization-induced migration of epidermal Langerhans cells to regional lymph nodes. *Cell Immunol.* **158**, 389-399.

Martin-Fontecha, A., Sebastiani, S., Hopken, U. E., Uguccioni, M., Lipp, M., Lanzavecchia, A. and Sallusto, F. (2003). Regulation of dendritic cell migration to the draining lymph node: impact on T lymphocyte traffic and priming. *J. Exp. Med.* **198**, 615-621.

Merad, M., Manz, M. G., Karsunky, H., Wagers, A., Peters, W., Charo, I., Weissman, I. L., Cyster, J. G. and Engleman, E. G. (2002). Langerhans cells renew in the skin throughout life under steady-state conditions. *Nat. Immunol.* **3**, 1135-1141.

Norose, K., Clark, J. I., Syed, N. A., Basu, A., Heber-Katz, E., Sage, E. H. and Howe, C. C. (1998). SPARC deficiency leads to early-onset cataractogenesis. *Invest. Ophthalmol. Vis. Sci.* **39**, 2674-2680.

Phanuphak, P., Moorhead, J. W. and Claman, H. N. (1974). Tolerance and contact sensitivity to DNFB in mice. I. In vivo detection by ear swelling and correlation with in vitro cell stimulation. *J. Immunol.* **112**, 115-123.

Price, A. A., Cumberbatch, M., Kimber, I. and Ager, A. (1997). alpha 6 integrins are required for Langerhans cell migration. *Adv. Exp. Med. Biol.* **417**, 129-132.

Puolakkainen, P., Bradshaw, A. D., Kyriakides, T. R., Reed, M., Brekken, R., Wight, T., Bornstein, P., Ratner, B. and Sage, E. H. (2003). Compromised production of extracellular matrix in mice lacking secreted protein, acidic and rich in cysteine (SPARC) leads to a reduced foreign body reaction to implanted biomaterials. *Am. J. Pathol.* **162**, 627-635.

Raines, E. W., Lane, T. F., Iruela-Arispe, M. L., Ross, R. and Sage, E. H.

(1992). The extracellular glycoprotein SPARC interacts with platelet-derived growth factor (PDGF)-AB and -BB and inhibits the binding of PDGF to its receptors. *Proc. Natl. Acad. Sci. USA* **89**, 1281-1285.

Randolph, G. J., Inaba, K., Robbiani, D. F., Steinman, R. M. and Muller, W. A. (1999). Differentiation of phagocytic monocytes into lymph node dendritic cells in vivo. *Immunity* **11**, 753-761.

Ratzinger, G., Stoitzner, P., Ebner, S., Lutz, M. B., Layton, G. T., Rainer, C., Senior, R. M., Shipley, J. M., Fritsch, P., Schuler, G. et al. (2002). Matrix metalloproteinases 9 and 2 are necessary for the migration of Langerhans cells and dermal dendritic cells from human and murine skin. *J. Immunol.* **168**, 4361-4371.

Rotta, G., Edwards, E. W., Sangaletti, S., Bennett, C., Ronzoni, S., Colombo, M. P., Steinman, R. M., Randolph, G. J. and Rescigno, M. (2003). Lipopolysaccharide or whole bacteria block the conversion of inflammatory monocytes into dendritic cells in vivo. *J. Exp. Med.* **198**, 1253-1263.

Sangaletti, S., Stoppacciaro, A., Guiducci, C., Torrisi, M. R. and Colombo, M. P. (2003). Leukocyte, Rather than Tumor-produced SPARC, Determines Stroma and Collagen Type IV Deposition in Mammary Carcinoma. *J. Exp. Med.* **198**, 1475-1485.

Savani, R. C., Zhou, Z., Arguiri, E., Wang, S., Vu, D., Howe, C. C. and DeLisser, H. M. (2000). Bleomycin-induced pulmonary injury in mice deficient in SPARC. *Am. J. Physiol. Lung. Cell Mol. Physiol.* **279**, L743-L750.

Schwarzenberger, K. and Udey, M. C. (1996). Contact allergens and epidermal proinflammatory cytokines modulate Langerhans cell E-cadherin expression in situ. *J. Invest. Dermatol.* **106**, 553-558.

Stoitzner, P., Zanella, M., Ortner, U., Lukas, M., Tagwerker, A., Janke, K., Lutz, M. B., Schuler, G., Echtenacher, B., Ryffel, B. et al. (1999). Migration of langerhans cells and dermal dendritic cells in skin organ cultures: augmentation by TNF-alpha and IL-1beta. *J. Leukoc. Biol.* **66**, 462-470.

Tang, A., Amagai, M., Granger, L. G., Stanley, J. R. and Udey, M. C. (1993). Adhesion of epidermal Langerhans cells to keratinocytes mediated by E-cadherin. *Nature* **361**, 82-85.

Tremble, P. M., Lane, T. F., Sage, E. H. and Werb, Z. (1993). SPARC, a secreted protein associated with morphogenesis and tissue remodeling, induces expression of metalloproteinases in fibroblasts through a novel extracellular matrix-dependent pathway. *J. Cell Biol.* **121**, 1433-1444.

Valladeau, J., Clair-Moninot, V., Dezutter-Dambuyant, C., Pin, J. J., Kissenpfennig, A., Mattei, M. G., Ait-Yahia, S., Bates, E. E., Malissen, B., Koch, F. et al. (2002). Identification of mouse langerin/CD207 in Langerhans cells and some dendritic cells of lymphoid tissues. *J. Immunol.* **168**, 782-792.

Weinlich, G., Heine, M., Stossel, H., Zanella, M., Stoitzner, P., Ortner, U., Smolle, J., Koch, F., Sepp, N. T., Schuler, G. et al. (1998). Entry into afferent lymphatics and maturation in situ of migrating murine cutaneous dendritic cells. *J. Invest. Dermatol.* **110**, 441-448.

Weiss, J. M., Sleeman, J., Renkl, A. C., Dittmar, H., Termeer, C. C., Taxis, S., Howells, N., Hofmann, M., Kohler, G., Schopf, E. et al. (1997). An essential role for CD44 variant isoforms in epidermal Langerhans cell and blood dendritic cell function. *J. Cell Biol.* **137**, 1137-1147.

Weiss, J. M., Renkl, A. C., Maier, C. S., Kimmig, M., Liaw, L., Ahrens, T., Kon, S., Maeda, M., Hotta, H., Uede, T. et al. (2001). Osteopontin is involved in the initiation of cutaneous contact hypersensitivity by inducing Langerhans and dendritic cell migration to lymph nodes. *J. Exp. Med.* **194**, 1219-1229.

Wewer, U. M., Albrechtsen, R., Fisher, L. W., Young, M. F. and Termine, J. D. (1988). Osteonectin/SPARC/BM-40 in human decidua and carcinoma, tissues characterized by de novo formation of basement membrane. *Am. J. Pathol.* **132**, 345-355.

Yan, Q., Clark, J. I., Wight, T. N. and Sage, E. H. (2002). Alterations in the lens capsule contribute to cataractogenesis in SPARC-null mice. *J. Cell Sci.* **115**, 2747-2756.

Yan, Q., Blake, D., Clark, J. I. and Sage, E. H. (2003). Expression of the matricellular protein SPARC in murine lens: SPARC is necessary for the structural integrity of the capsular basement membrane. *J. Histochem. Cytochem.* **51**, 503-511.